Int Ophthalmol
https://doi.org/10.1007/s10792-022-02382-7

ORIGINAL PAPER

Changes in retinal and choroidal capillary dynamics in patients with multisystem inflammatory syndrome in children

Tuğba Kurumoğlu Incekalan · Umit Celik · Orkun Tolunay · Goksu Hande Naz Şimdivar · Emine Alyamaç Sukgen

Received: 29 October 2021 / Accepted: 14 June 2022

Abstract

Purpose To evaluate patients with multisystemic inflammatory syndrome in children (MIS-C) associated with severe acute respiratory syndrome coronavirus 2 (SARS-CoV-2) infection using optical coherence tomography angiography (OCTA) during and after resolution of inflammation to investigate the effect of this entity on the retinal and choroidal circulation.

Methods The study included 38 eyes of 19 patients diagnosed as having MIS-C between March 2021 and June 2021. OCTA measurements of choroidal thickness and vessel density in the radial peripapillary capillary plexus (RPCP), superficial capillary plexus (SCP), and deep capillary plexus (DCP) obtained at time of diagnosis and 60 days later were compared. Correlations between C-reactive protein (CRP) levels at diagnosis and retinochoroidal involvement were investigated.

Results Compared to post-recovery follow-up examinations, patients with active MIS-C showed foveal avascular zone enlargement ($p=0.031$), decreased vessel density in the temporal parafoveal SCP ($p=0.047$) and all parafoveal areas of the DCP ($p<0.05$ for all), and increased choroidal thickness ($p=0.021$). Correlation analysis between CRP levels and OCTA changes during MIS-C revealed significant negative correlations with all parafoveal sectors of the SCP and DCP and a significant positive correlation with CT.

Conclusion There were especially marked effects on the DCP and choroid in MIS-C patients. Our findings also correlate with CRP levels. The use of optical coherence tomography angiography in patients with multisystemic inflammatory syndrome may have potential future implications for detecting ocular microvascular changes that occur before permanent damage develops.

Clinical Trial Registration Number and Date: 77/1340; March 1, 2021.

T. Kurumoğlu Incekalan (✉) · G. H. Naz Şimdivar · E. Alyamaç Sukgen
Depertmant of Opthalmology, Adana City Training and Research Hospital, University of Health Sciences, Adana, Turkey
e-mail: tugbakurumoglu@hotmail.com

G. H. Naz Şimdivar
e-mail: drghande@gmail.com

E. Alyamaç Sukgen
e-mail: esukgen@gmail.com

U. Celik · O. Tolunay
Pediatric Infectious Diseases, Adana City Training and Research Hospital, University of Health Sciences, Adana, Turkey
e-mail: ucelik32@gmail.com

O. Tolunay
e-mail: orkuntolunay@yahoo.co.uk

Published online: 29 August 2022

Keywords Children · Multisystem inflammatory syndrome in children (MIS-C) · Retina · SARS-CoV-2 · Optical coherence tomography angiography

Introduction

Severe acute respiratory syndrome coronavirus 2 (SARS-CoV-2) infection has led to a global pandemic with significant morbidity and mortality [1]. In children, the disease had a good prognosis according to initial reports. More than half of pediatric SARS-CoV-2 patients were asymptomatic or experienced mild symptoms [2, 3] However, later, new cases with hyperinflammatory findings and hemodynamic shock and Kawasaki-like clinic were reported [4–7]. This new entity was named multisystem inflammatory syndrome in children (MIS-C) by The United States Centers for Disease Control and Prevention (CDC) in May 2020 [8]

MIS-C is considered a rare complication of SARS-CoV-2 infection. It was reported that the incidence of SARS-CoV-2 infection in people younger than 21 years of age was 322 in 100,000, while the incidence of MIS-C cases in the same period was 2 in 100,000 [9]. The median age of patients with MIS-C is 9 years (6 months–20 years)[10]. The most common clinical manifestations are fever, tachycardia, hypotension, gastrointestinal symptoms (abdominal pain, diarrhea), rash, conjunctivitis or conjunctival injection, cheilitis and/or strawberry tongue, and edema/erythema of the extremities. Acute phase reactants such as C-reactive protein (CRP), interleukin 6 (IL6), procalcitonin, fibrinogen, D-dimer, lactate dehydrogenase (LDH) and ferritin values are elevated. Major complications of the disease include respiratory distress requiring mechanical ventilation, myocardial dysfunction requiring aggressive treatment, and acute kidney injury [10]. The mortality rate was reported to be 1.4%. MIS-C is believed to occur due to an abnormal immune response, as in macrophage activation syndrome or Kawasaki disease, but the mechanism triggering this abnormal response is not clearly known. The fact that most affected children have negative RT-PCR results but positive antibodies evincing previous infection suggests that the cause of MIS-C is a specific inflammatory response following SARS-CoV-2 infection [6, 10–12].

Optical coherence tomography angiography (OCTA) is a noninvasive method that produces vascular flow maps of the retina and choroid, thereby creating a three-dimensional image of the retinal microvasculature. Various studies have shown that OCTA offers a reliable method for the qualitative and quantitative assessment of pathological or physiological changes in the retinal, choroidal, and optic nerve vasculature [13–15]. The retina and choroid are among the most energy-demanding tissues in the body and are very sensitive to ischemia [16, 17]. Various studies have indicated that retinal vessel density and retinal perfusion reflect systemic hemodynamic changes and systemic inflammatory response [18–20]. The choroid has the highest blood flow per unit mass of any tissue in the body. Due to its high vascularity, this layer is sensitive to inflammation in multisystemic diseases and is primarily affected in systemic vascular disorders [17]. Retinal and choroidal thickness has recently been proposed as potential inflammatory biomarkers, especially for inflammatory diseases with vascular involvement [21–23]. In this study, we aimed to investigate microvascular changes in the retina and choroid in the newly defined entity COVID-19-associated MIS-C and evaluate the correlation between these changes and inflammation severity as assessed by CRP level. To the best of our knowledge, this study is the first in the literature to investigate retinochoroidal vascular changes in children with MIS-C.

Materials and methods

This prospective study was conducted at the ophthalmology clinic of a tertiary care training hospital. The study protocol was approved by the institutional ethics committee. The study was performed in accordance with the tenets of the Declaration of Helsinki, and written informed consent forms were obtained from all participants and the parents of underage participants.

Patient selection and inclusion criteria

Patients aged 6–18 years who met the criteria for MIS-C associated with COVID-19 and were treated in the pediatric wards of our hospital between March 2021 and June 2021 were evaluated. Patients whose

parents or legal representatives agreed to their participation in the study and provided consent were included. Real-time reverse transcription polymerase chain reaction (RT-PCR) testing (of nasopharyngeal swab samples) and antigen test were used as laboratory evidence of SARS-CoV-2 infection. The US Centers for Disease Control and Prevention (CDC) criteria [24] were used to diagnose MIS-C. The CDC definition of MIS-C is as follows:

- Age < 21 years.
- No alternative plausible diagnoses.
- Positive for current or recent SARS-CoV-2 infection by RT-PCR, serology, or antigen test; or COVID-19 exposure within the 4 weeks before symptom onset.
- Presenting with fever (body temperature > 38.0 °C for ≥ 24 h, or report of subjective fever lasting ≥ 24 h).
- Laboratory evidence of inflammation demonstrated by one or more of the following: elevated C-reactive protein (CRP), erythrocyte sedimentation rate (ESR), procalcitonin, fibrinogen, ferritin, D-dimer, lactic acid dehydrogenase (LDH), or interleukin 6 (IL-6) level, elevated neutrophil count, reduced lymphocyte count, and low albumin level.
- Evidence of clinically severe illness requiring hospitalization, with multisystem (> 2) organ involvement (cardiac, renal, respiratory, hematologic, gastrointestinal, dermatologic or neurological).

Exclusion criteria

Patients with any congenital or systemic disease, regular medication use, or severe clinical condition requiring more aggressive treatment than the standard treatment for MIS-C were not included. Ocular exclusion criteria were any chorioretinal disease, optic disk pathology, strabismus, or amblyopia; previous eye surgery or trauma; medical history of prematurity; history of any autoimmune or systemic disorder (e.g., diabetes mellitus, hypertension); refractive error greater than 4.00 D; intraocular pressure higher than 21 mmHg; and ocular media opacities that reduced OCTA image quality.

Measurements were repeated for patients with poor image quality due to eye movement or poor fixation. Only images with a signal strength index of 7 or greater were included in the study.

Ocular assessment

All participants underwent a full ophthalmological examination including autorefraction (Tonoref III; Nidek Co. Ltd), best-corrected visual activity (Snellen chart), intraocular pressure measurement with an air-puff tonometer (Tonoref III), slit-lamp examination, and dilated funduscopy. Macular and peripapillary vessel density and foveal avascular zone (FAZ) measurements were performed during the same time of day (between 9 AM and 12 PM) using the AngioVue software of the OCTA device (Optovue RTVue XR Avanti; Optovue Inc., Fremont, CA) after pupil dilation (1% tropicamide). All measurements were made by the same technician who was trained in the use of the device. The same examinations were performed at time of diagnosis and 60 days later. The right eye of all participants was evaluated.

OCTA examination was performed using the standard macular and peripapillary protocol. All eye scans were obtained using a 3 × 3 mm scanning area centered on the fovea and a 4.5 × 4.5 mm scanning area centered on the optic disk. The eye-tracking function was active during the scans, and motion correction was applied to minimize motion artifacts arising from microsaccades and fixation changes.

The foveal avascular zone (FAZ) is the retinal capillary-free area located in the central fovea. FAZ area was measured using the 'retina' tool of the software, which delineates it automatically. FAZ measurement by OCTA is shown in Fig. 1. Parafoveal vessel density was calculated for the annular area between 0.3 and 1.25 mm radius from the center of the macula. The parafoveal region was divided into four sectors of 90 degrees each (temporal, superior, nasal, and inferior), and the vessel density in each sector was calculated. The en face images of the SCP were segmented between an inner border 3 µm below the internal limiting membrane and an outer border 15 µm below the inner plexiform layer (IPL). En face images of the DCP were segmented under the IPL with inner and outer boundaries at 15 and 70 µm, respectively. Peripapillary capillary vessel density was measured in a 1.00-mm wide elliptical ring extending outward from the optic disk border in the radial peripapillary capillary plexus (RPCP). The RPCP extends from the

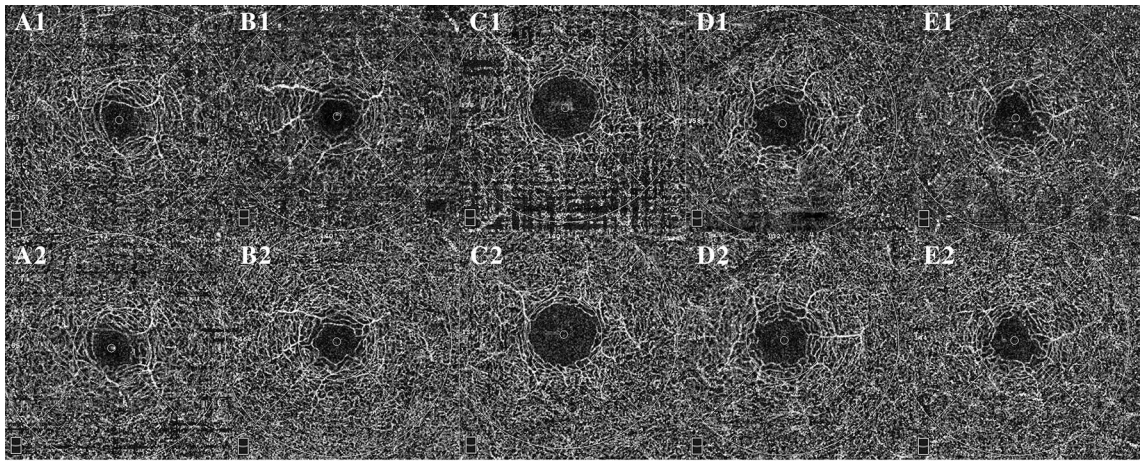

Fig. 1 En face optical coherence tomography angiograms segmented at the level of the deep retinal capillary plexus from 5 MIS-C patients at diagnosis (**A1**–**E1**) and 60 days later (**A2**–**E2**)

internal limiting membrane to the nerve fiber layer. Vessel densities of the whole image, inside disk, and peripapillary areas were examined.

Peripapillary retinal nerve fiber layer (ppRNFL) thickness was assessed in the 3.45-mm-diameter circle around the optic disk in the optic nerve head mode. Subfoveal choroidal thickness (CT) was measured manually between the hyperreflective line of Bruch's membrane and the innermost hyperreflective line of the choroidoscleral interface. Subfoveal choroidal thickness measurements were made by two researchers by masking who and which measurement the image belonged to. The final thickness for analysis was calculated by taking the average of the two investigators.

Image quality was assessed for all OCTA scans. Poor-quality images, defined as scans with quality index < 7, and images with residual motion artifacts or segmentation errors were excluded from the analysis.

Statistical analysis

Statistical analysis of the data was performed using the SPSS version 21.0 package program. Descriptive statistics were calculated as mean ± standard deviation for normally distributed numerical variables and median and interquartile range (IQR) for non-normally distributed variables. Categorical variables were expressed as count (n) and percentage (%). Continuous variables were checked for normality using Shapiro–Wilk test. Before and after comparisons were performed using paired t-test for normally distributed variables and Wilcoxon test for non-normally distributed variables. Spearman and Pearson correlation coefficients were calculated to examine the linear relationships between continuous variables. The level of statistical significance was accepted as $p < 0.05$.

Results

Twenty-one eyes of 21 patients meeting the MIS-C diagnostic criteria were included in the study. In tests performed to confirm that MIS-C was associated with COVID-19, all patients had a negative nasopharyngeal swab RT-PCR test, while all had a positive antigen test. The study group consisted of 12 girls (57.2%) and 9 boys (42.8%), with a mean age of 11.64 ± 2.79 (6–16) years. Data pertaining to the patients' systemic involvement and treatment they received are summarized in Table 1.

In examinations performed at time of diagnosis, best-corrected visual acuity (BCVA) 20/20 or better for all participants, all patients had normal intraocular pressures, and normal anterior and posterior segment findings in detailed ophthalmological examinations. The initial examination revealed no ocular findings in any patient.

When we compared the OCTA data at the time of diagnosis, we found that the FAZ region was larger ($p = 0.031$) and the choroidal thickness was greater

Table 1 Clinical characteristics and treatment of MIS-C patients

Clinical data	*n* (%)
Fever	19 (100)
Gastrointestinal involvement	18 (94.7)
Mucocutaneous involvement	11 (42.1)
Cardiac involvement	6 (31.6)
Respiratory involvement	5 (26.3)
Neurologic involvement	1 (5.3)
Intravenous immunoglobulin therapy	18 (94.7)
Steroid therapy	16 (84.2)
Anticoagulant therapy	19 (100)
Positive inotrope therapy	5 (26.3)
Intensive care	7 (36.8)
Mean length of hospital stay (days), mean ± SD	11.6 ± 4.13

($p = 0.021$) than the data repeated 60 days later. SCP vessel density values showed that temporal parafoveal vessel density was lower during the acute period than at 60 days follow-up ($p = 0.047$). There were no statistically significant differences in SCP vessel density in the other parafoveal sectors and fovea. (Table 2).

In terms of the DCP, we found that vessel density values did not differ in the fovea but were significantly lower in the acute period in all parafoveal regions except the inferior sector. (Table 2). Figure 1 shows segmented optical coherence tomography angiograms at the deep retinal capillary plexus level taken from 5 MIS-C patients at diagnosis (A1–E1) and 60 days later (A2-E2). The increase in vessel density in DCP after recovery is remarkable.

In our comparisons of the ppRNFL and RPCP vessel density values in the acute period of MIS-C and after recovery, there were no significant changes in ppRNFL thickness or RPCP vessel density with the exception of a significant decrease in the inside disk region ($p < 0.001$) (Table 3).

To evaluate inflammation severity, we assessed levels of the acute phase reactant CRP and compared them with vessel density parameters. The mean CRP level at time of diagnosis in the MIS-C patients included in the study was 206.91 ± 102.5 (4–415) mg/L (normal reference range for CRP: 0–5 mg/L). When we examined the changes in the acute period based on post-discharge follow-up examinations, we observed no correlation between CRP and FAZ area,

Table 2 CT, FAZ, SCP-VD, and DCP-VD measurements in MIS-C patients during and after the acute period

	At diagnosis		60-day follow-up		*p*
	Mean ± SD	Median (IQR)	mean ± SD	Median (IQR)	
CT	301.86 ± 27.9	300 (286.25–324.5)	279.5 ± 30.3	274.5 (262.75–285.75)	**0.021***
FAZ	0.30 ± 0.08	0.3 (0.25–0.32)	0.28 ± 0.08	0.29 (0.24–0.31)	**0.031**
SCP-VD					
Fovea	16.5 ± 4.57	15.5 (12.63–19.03)	17.01 ± 5.82	16.1 (13.03–19.65)	0.051
Parafovea	51.02 ± 2.81	51.1 (49.18–53.28)	51.23 ± 2.29	51 (50.03–52.65)	0.302*
Temporal	49.51 ± 3.04	49 (47.65–51.93)	49.94 ± 2.63	49.65 (48.25–51.85)	**0.047***
Superior	53.16 ± 2.36	52.8 (51.38–55.1)	52.87 ± 3.33	52.8 (50.23–55.5)	0.114*
Nasal	50 ± 3.17	49.75 (48.48–52.85)	50.44 ± 2.71	50.7 (49.13–52.45)	0.834
Inferior	51.81 ± 3.4	52.35 (49.65–54.48)	51.96 ± 2.81	52.5 (49.65–54.15)	0.852
DCP-VD					
Fovea	33.92 ± 7.13	35.7 (30.48–36.98)	34.01 ± 7.62	36.1 (31.15–38.35)	0.085
Parafovea	57.08 ± 4.21	58.1 (55.4–59.58)	58.20 ± 3.06	58.55 (56.1–60.53)	**0.003**
Temporal	57.07 ± 4.40	57.75 (55.13–59.93)	58.56 ± 3.13	58.85 (56.75–60.95)	**< 0.001**
Superior	57.45 ± 4.26	58.35 (55.83–61.18)	58.84 ± 3.19	59.1 (57.38–60.88)	**< 0.001**
Nasal	57.15 ± 5.10	58.4 (55.33–60.48)	58.55 ± 2.99	59 (56.73–60.2)	**0.016**
Inferior	56.50 ± 4.69	57.3 (54.83–59.25)	57.79 ± 3.28	57.9 (55.2–60.18)	0.102

p: Wilcoxon test *Paired *t*-test. Values are presented as mean ± standard deviation and median and interquartile range (IQR). Bold values indicate statistical significance. $p < .05$. CT: Subfoveal choroidal thickness, FAZ: Foveal avascular zone, SCP-VD: Superficial capillary plexus vessel density, DCP-VD: Deep capillary plexus vessel density

Table 3 Peripapillary RNFL and RPCP-VD measurements in MIS-C patients during and after the acute period

	At diagnosis		60-day follow-up		*p*
	Mean ± SD	Median (IQR)	Mean ± SD	Median (IQR)	
ppRNFLT					
Mean	106.16 ± 14.82	102.5 (98–108.75)	105 ± 13.44	101 (98–109.75)	0.162
Superior Hemi	106.09 ± 15.26	103.5 (98–112)	104.86 ± 14.16	103.5 (96.25–109.75)	0.119
Inferior Hemi	106.25 ± 14.88	103 (98–109.75)	105.48 ± 13.63	101.5 (98–110)	0.176
RPCP-VD					
Whole image	50.27 ± 2.26	49.7 (48.83–51.8)	50.75 ± 2.56	50.95 (48.75–52.43)	0.081*
Superior Hemi	52.27 ± 3.06	52.2 (49.6–54.58)	52.88 ± 3.28	53.15 (50.13–55.05)	0.118*
Inferior Hemi	51.99 ± 3.29	51.6 (49.4–54.4)	52.64 ± 2.94	52.8 (50.13–54.35)	0.153*
Inside disk	58.57 ± 42.79	52.85 (50.18–55.15)	54.21 ± 2.81	54.55 (52.33–56.25)	< 0.001

p: Wilcoxon test *Paired *t*-test; values are presented as mean ± standard deviation and median and interquartile range (IQR) ppRNFLT: PERİPAPİLLARY retinal nerve fiber layer thickness, RPCP-VD: Radial peripapillary capillary plexus vessel density

ppRNFL thickness, or vessel density in the RPCP or foveal areas of the SCP and DCP. There was a significant negative correlation between CRP and vessel density in all parafoveal sectors of the SCP and DCP. Also, there was a positive correlation between CRP and CT. (Table 4).

Discussion

Although initially mysterious, emerging data suggest that MIS-C is a post-infectious (SARS-CoV-2) hyperinflammatory disease caused by an abnormal immune response. In addition, the growing number of MIS-C cases and case series reported from all over the world show that MIS-C is more common than it first seemed. Although rare and treatable, delays in diagnosis and treatment can result in morbidity and mortality.

The presence of angiotensin-converting enzyme (ACE), the main receptor to which the S protein of SARS-CoV-2 binds in order to enter cells, has been demonstrated in the cell membranes of type II alveolar cells in the lungs, enterocytes of the small intestine, vascular smooth muscle cells, and the arterial smooth muscle cells of most organs [25, 26]. These receptors have also been found in various types of cells in the retina and choroid, including Müller cells, ganglion cells, retinal vascular endothelial cells, and photoreceptor cells [27]. Receptor-mediated viral entry into cells results in macrophage and complement activation, cytokine

Table 4 The relationship between CRP level at diagnosis and relative changes in OCTA parameters in MIS-C patients

	r	*p*
SCP-VD		
Foveal	− 0.090	0.560
Parafoveal	− 0.308	**0.042***
Temporal	− 0.441	**0.003***
Superior	− 0.388	**0.009**
Nasal	− 0.321	**0.034**
Inferior	− 0.335	**0.026***
DCP-VD		
Foveal	− 0.269	0.077
Parafoveal	− 0.753	**< 0.001**
Temporal	− 0.674	**< 0.001**
Superior	− 0.638	**< 0.001**
Nasal	− 0.480	**0.001**
Inferior	− 0.503	**0.001**
FAZ	0.114	0.459
ppRNFLT mean	0.026	0.867*
ppRNFLT superior	0.154	0.319
ppRNFLT inferior	− 0.019	0.901*
RPCP-VD whole image	0.015	0.922*
RPCP-VD superior	− 0.010	0.950*
RPCP-VD inferior	− 0.240	0.117
RPCP-VD inside disk	0.066	0.669
CT	0.434	**0.003**

p: Spearman rho *Pearson correlation; Relative change: (During-After)/During × 100, DCP: Deep capillary plexus, ppRNFLT: Peripapillary retinal nerve fiber layer thickness, RPCP-VD: Radial peripapillary capillary plexus vessel density, SCP-VD: Superficial capillary plexus vessel density, DCP-VD: Deep capillary plexus vessel density. Bold values indicate statistical significance ($p < .05$)

release, endothelial damage, thrombotic microangiopathy, and subsequent ischemia. This is the main mechanism of action of the virus, but it is not known what triggers the late and abnormal immune response seen in MIS-C patients approximately 4–6 weeks after active infection. However, this late complication of SARS-CoV-2 infection has the potential to cause impaired blood flow in the retina and choroid.

Numerous studies have shown that OCTA may have an important role in the early diagnosis and assessment of the severity of systemic vascular and inflammatory diseases [28–31]. In this study, we aimed to evaluate changes in the microvascular structure of the retina and choroid in MIS-C patients using OCTA.

Our analysis of vascular changes in the macular region during the acute phase of MIS-C revealed significant FAZ enlargement. Due to the absence of retinal vessels in the FAZ, the underlying choriocapillaris is solely responsible for supplying the cone cells [32]. As a result, the FAZ is particularly sensitive to ischemic events and can thus act as an indicator of various pathological processes [33]. Abrishami et al. [34] also reported in their study of adults that FAZ area was larger in the COVID-19 group, but the difference did not reach statistical significance. Similarly, Türker et al. [35] reported that FAZ area was increased but not significantly in patients with COVID-19. However, both studies included patients after the recovery period. This difference may also be attributed to a more intense inflammatory process in children with MIS-C.

When we looked at the changes in vessel density in the SCP and DCP, we observed decreases in both layers, but those in the DCP were more statistically significant. Abrishami et al. [34] also detected significant reductions in vessel density in both the SCP and DCP in adults with COVID-19. Türker et al. [35] reported that the DCP was more affected, similar to our findings, and choroidal blood flow was increased. Several factors may make the DCP more susceptible to damage, including its distance from the larger arterioles, proximity to the high metabolic demand of the outer retina, and complex vascular anatomical architecture [36]. Similarly, the high metabolic activity and complex vascular structure of the outer retina may make it more susceptible to poor perfusion caused by generalized vasospasm.

As a limitation of our study, since there was no software to measure the choroidal vascularity index in our OCTA device, choroidal blood supply was evaluated indirectly through choroidal thickness. Subfoveal CT measurements may be an indirect indicator of subfoveal ocular perfusion [37]. Hayreh et al. [38] showed that hypercapnia had a vasodilatory effect on the choroidal circulation. The increase in choriocapillaris flow in the study may have been a hypoxia-induced vasodilation response due to ischemia of the choroidal tissue feeding the outer retinal layers [35]. In a review examining retinal and choroidal involvement in systemic inflammation and autoimmune diseases, choroidal thickness was reported to decrease in some studies and increase in others [39]. It was concluded that choroidal thickening occurs during exacerbations of these diseases, while atrophy and fibrosis caused by repeated episodes during the chronic process result in choroidal thinning. Subclinical choroidal infiltration due to inflammatory mediators released as a result of systemic inflammation may cause hyperpermeability [17]. The choroid is not autoregulated like the retina; therefore, it is more susceptible to systemic changes.

We did not detect any significant changes in RPCP parameters (except in the inside disk area) or ppRNFL thickness values in patients with MIS-C. This may suggest that the peripapillary region is less sensitive to changes associated with systemic inflammation. The mean length of hospital stay in our study was 11.6 days. The fact that these patients' clinical and inflammation parameters largely regressed leading up to discharge suggests that the process was not severe enough to affect the peripapillary region.

CRP is the blood inflammation marker most frequently elevated in MIS-C patients (94% of patients) [40]. Similarly, CRP values were high in all but one of our patients (mean 206.91 ± 102.5 mg/L). Therefore, we used CRP values to examine the relationship between inflammation severity and retinochoroidal vascular involvement. We determined that high CRP levels were correlated with vascular involvement in all parafoveal quadrants in both the superficial and deep retinal plexuses and the choroid.

The most important limitation of our study is the small sample size. Due to the insufficient normative data for children and the small number of patients evaluated, we did not think that matching with healthy children would provide an optimal

comparison. Therefore, we compared the MIS-C patients' acute findings with follow-up measurements obtained after clinical and laboratory recovery. Although the patients exhibited clinical and laboratory resolution in follow-up examinations, we do not know whether they had any persistent changes in retinal vascular structure compared to healthy children. Another limitation is that image quality has been shown to affect vessel density analysis in OCTA [41, 42]. Although images with a signal strength index lower than 7 were not included in the analysis, the fact that the patients were children and were in poor clinical condition during the acute phase of the disease may have affected our results. None of our patients had very severe systemic involvement requiring prolonged hospitalization. A more extensive vascular effect may have been observed in the presence of more severe inflammation and systemic involvement. Nevertheless, our results may indicate that the DCP and choroid are particularly affected in MIS-C patients. The fact that the changes are largely correlated with CRP levels may suggest that ocular involvement is proportional to the severity of inflammation. Our results demonstrated a decrease in vessel density, especially in the DCP, and an increase in choroidal thickness. The changes were largely correlated with CRP levels. Multicenter studies with more patients are needed to understand the systemic and local changes caused by this hyperinflammatory response in children after SARS-CoV-2 infection.

Acknowledgements This work was done at University of Health Sciences Adana City Training and Research Hospital (a tertiary care training hospital).

Author contributions All authors contributed to the study conception and design. TKİ had the original idea. GHNŞ, TİK, OT, UÇ and EAS performed the data collection, initial literature review and drafted the article. TİK, UÇ and OT provided direction and senior support, additional literature input and revised the article into the final version. All authors read and approved the final manuscript.

Funding No funding was received for this research.

Declarations

Conflict of ınterest All authors certify that they have no affiliations with or involvement in any organization or entity with any financial interest, or non-financial interest in the subject matter or materials discussed in this manuscript.

Ethical approval All procedures performed in studies involving human participants were in accordance with the ethical standards of the (place name of institution and/or national research committee) and with the 1964 Helsinki declaration and its later amendments or comparable ethical standards.

Informed consent Informed consent was obtained from all participants and the parents of underage participants.

References

1. Toraih EA, Hussein MH, Elshazli RM, Kline A, Munshi R, Sultana N, Taghavi S, Killackey M, Duchesne J, Fawzy MS, Kandil E (2021) Multisystem inflammatory syndrome in pediatric COVID-19 patients: a meta-analysis. World J Pediatr 17(2):141–151. https://doi.org/10.1007/s12519-021-00419-y
2. Dong Y, Mo X, Yl Hu et al (2020) Epidemiology of COVID-19 among children in China. Pediatrics 145(6):e20200702. https://doi.org/10.1542/peds.2020-0702
3. Mustafa NM, Selim LA (2020) Characterisation of COVID-19 pandemic in paediatric age group: a systematic review and meta-analysis. J Clin Virol 128:104395. https://doi.org/10.1016/j.jcv.2020.104395
4. Riphagen S, Gomez X, CGonzalez-Martinez C et al (2020) Hyperinflammatory shock in children during COVID-19 pandemic. Lancet 395(10237):1607–1608. https://doi.org/10.1016/S0140-6736(20)31094-1
5. Pain CE, Felsenstein S, Gl C et al (2020) Novel paediatric presentation of COVID-19 with ARDS and cytokine storm syndrome without respiratory symptoms. Lancet Rheumatol 2(7):e376–e379. https://doi.org/10.1016/S2665-9913(20)30137-5
6. Verdoni L, Mazza A, Al G et al (2020) An outbreak of severe Kawasaki-like disease at the Italian epicentre of the SARS-CoV-2 epidemic: an observational cohort study. Lancet 395(10239):1771–1778. https://doi.org/10.1016/S0140-6736(20)31103-X
7. DeBiasi RL, Song X, Ml D et al (2020) Severe coronavirus disease-2019 in children and young adults in the Washington, DC. Metropolitan Region J Pediatr 223:199-203.e1. https://doi.org/10.1016/j.jpeds.2020.05.007
8. -Centers for Disease Control and Prevention. Emergency preparedness and response. https://emergency.cdc.gov/han/2020/han00432.asp. Accessed May 22, 2020
9. Dufort EM, Koumans EH, Chow EJ et al (2020) New York State and centers for disease control and prevention multisystem inflammatory syndrome in children investigation team: multisystem inflammatory syndrome in children in New York State. N Engl J Med 383(4):347–358. https://doi.org/10.1056/NEJMoa2021756
10. Aronoff SC, Hall A, Del Vecchio MT (2020) The natural history of severe acute respiratory syndrome coronavirus 2-related multisystem inflammatory syndrome in children: a systematic review. J Pediatric Infect Dis Soc 9(6):746–751. https://doi.org/10.1093/jpids/piaa112

11. Dolinger MT, Person H, Rl S et al (2020) Pediatric crohn disease and multisystem inflammatory syndrome in children (MIS-C) and COVID-19 treated with infliximab. J Pediatr Gastroenterol Nutr 71(2):153–155. https://doi.org/10.1097/MPG.0000000000002809
12. Chiotos K, Bassiri H, Behrens EM et al (2020) Multisystem ınflammatory syndrome in children during the coronavirus 2019 pandemic: a case series. J Pediatric Infect Dis Soc 9(3):393–398. https://doi.org/10.1093/jpids/piaa069
13. Jia Y, Bailey ST, Wilson DJ et al (2014) Quantitative optical coherence tomography angiography of choroidal neovascularization in age-related macular degeneration. Ophthalmology 121(7):1435–1444. https://doi.org/10.1016/j.ophtha.2014.01.034
14. Couturier A, Mané V, Sl B et al (2015) Capillary plexus anomalies in diabetic retinopathy on optical coherence tomography angiography. Retina 35(11):2384–2391. https://doi.org/10.1097/IAE.0000000000000859
15. Coscas F, Glacet-Bernard A, Miere A et al (2016) Optical coherence tomography angiography in retinal vein occlusion: evaluation of superficial and deep capillary plexa. Am J Ophthalmol 161:160-711.e2. https://doi.org/10.1016/j.ajo.2015.10.008
16. Nakaizumi A, Puro DG (2011) Vulnerability of the retinal microvasculature to hypoxia: role of polyamine-regulated KATP channels. Invest Ophthalmol Vis Sci 52:9345–9352. https://doi.org/10.1167/iovs.11-8176
17. Ferreira CS, Beato J, Falcão MS et al (2017) Choroidal thickness in multisystemic autoimmune diseases without ophthalmologic manifestations. Retina 37(3):529–535. https://doi.org/10.1097/IAE.0000000000001193
18. Nakayama LF, Bergamo VC, Conti ML et al (2019) The retinal foveal avascular zone as a systemic biomarker to evaluate inflammatory bowel disease control. Int J Retina Vitreous 5:16. https://doi.org/10.1186/s40942-019-0168-9
19. Arnould L, Guenancia C, Al A et al (2018) The EYE-MI pilot study: a prospective acute coronary syndrome cohort evaluated with retinal optical coherence tomography angiography. Invest Ophthalmol Vis Sci 59(10):4299–4306. https://doi.org/10.1167/iovs.18-24090
20. Kılınç Hekimsoy H, Şekeroğlu MA, Koçer AM et al (2020) Analysis of retinal and choroidal microvasculature in systemic sclerosis: an optical coherence tomography angiography study. Eye 34(4):763–770. https://doi.org/10.1038/s41433-019-0591-z
21. Altinkaynak H, Duru N, Uysal BS et al (2016) Choroidal thickness in patients with systemic lupus erythematosus analyzed by spectral-domain optical coherence tomography. Ocul Immunol Inflamm 24(3):254–260. https://doi.org/10.3109/09273948.2015.1006790
22. Coskun E, Gurler B, Yl P et al (2013) Enhanced depth imaging optical coherence tomography findings in Behçet disease. Ocul Immunol Inflamm 21(6):440–445. https://doi.org/10.3109/09273948.2013.817591
23. Duru N, Altinkaynak H, Şl E et al (2016) Thinning of choroidal thickness in patients with rheumatoid arthritis unrelated to disease activity. Ocul Immunol Inflamm 24(3):246–253. https://doi.org/10.3109/09273948.2015.1024329
24. Centers for Disease Control and Prevention Health Alert Network (HAN). Multisystem Inflammatory Syndrome in Children (MIS-C) Associated with Coronavirus Disease 2019 (COVID-19). https://emergency.cdc.gov/han/2020/han00432.asp. Accessed 05 May 2021
25. Hamming I, Timens W, Bulthuis ML et al (2004) Tissue distribution of ACE2 protein, the functional receptor for SARS coronavirus: a first step in understanding SARS pathogenesis. J Pathol 203(2):631–637. https://doi.org/10.1002/path.1570
26. Chamsi-Pasha MA, Shao Z, Tang WH (2014) Angiotensin-converting enzyme 2 as a therapeutic target for heart failure. Curr Heart Fail Rep 11(1):58–63. https://doi.org/10.1007/s11897-013-0178-0
27. Choudhary R, Kapoor MS, Al S et al (2016) Therapeutic targets of renin-angiotensin system in ocular disorders. J Curr Ophthalmol 29(1):7–16. https://doi.org/10.1016/j.joco.2016.09.009
28. Ikram MK, Cheung CY, Ml L, NIH/JDRF Workshop on Retinal Biomarker for Diabetes Group et al (2013) Retinal vascular caliber as a biomarker for diabetes microvascular complications. Diabetes Care 36(3):750–759. https://doi.org/10.2337/dc12-1554
29. Seidelmann SB, Claggett B, Bravo PE et al (2016) Retinal vessel calibers in predicting long-term cardiovascular outcomes: the atherosclerosis risk in communities study. Circulation 134(18):1328–1338. https://doi.org/10.1161/CIRCULATIONAHA.116.023425
30. Frost S, Kanagasingam Y, Sohrabi H, Vignarajan J, AIBL Research Group et al (2013) Retinal vascular biomarkers for early detection and monitoring of Alzheimer's disease. Transl Psychiatry 3(2):e233. https://doi.org/10.1038/tp.2012.150
31. De Silva DA, Manzano JJ, Liu EY, Woon FP et al (2011) Multi-centre retinal stroke study group: retinal microvascular changes and subsequent vascular events after ischemic stroke. Neurology 77(9):896–903. https://doi.org/10.1212/WNL.0b013e31822c623b
32. Snell R, Lemp M (1998) Clinical anatomy of the eye, 2nd edn. Blackwell Science Inc., Oxford
33. Samara WA, Say EA, Khoo CT, Higgins TP et al (2015) Correlation of foveal avascular zone size with foveal morphology in normal eyes using optical coherence tomography angiography. Retina 35(11):2188–2195. https://doi.org/10.1097/IAE.0000000000000847
34. Abrishami M, Emamverdian Z, Nl S et al (2021) Optical coherence tomography angiography analysis of the retina in patients recovered from COVID-19: a case-control study. Can J Ophthalmol 56(1):24–30. https://doi.org/10.1016/j.jcjo.2020.11.006
35. Turker IC, Dogan CU, Dl G et al (2021) Optical coherence tomography angiography findings in patients with COVID-19. Can J Ophthalmol 56(2):83–87. https://doi.org/10.1016/j.jcjo.2020.12.021
36. Nakahara T, Hoshino M, Hoshino S, Al M et al (2015) Structural and functional changes in retinal vasculature induced by retinal ischemia-reperfusion in rats. Exp Eye Res 135:134–145. https://doi.org/10.1016/j.exer.2015.02.020
37. Kim M, Kim SS, Kwon HJ et al (2012) Association between choroidal thickness and ocular perfusion pressure

in young, healthy subjects: enhanced depth imaging optical coherence tomography study. Invest Ophthalmol Vis Sci 53(12):7710–7717. https://doi.org/10.1167/iovs.12-10464
38. Hayreh SS (1990) In vivo choroidal circulation and its watershed zones. Eye 4(Pt 2):273–289. https://doi.org/10.1038/eye.1990.39
39. Steiner M, Esteban-Ortega MDM, Muñoz-Fernández S (2019) Choroidal and retinal thickness in systemic autoimmune and inflammatory diseases: a review. Surv Ophthalmol 64(6):757–769. https://doi.org/10.1016/j.survophthal.2019.04.007
40. Radia T, Williams N, Pl A et al (2021) Multi-system inflammatory syndrome in children & adolescents (MIS-C): a systematic review of clinical features and presentation. Paediatr Respir Rev 38:51–57. https://doi.org/10.1016/j.prrv.2020.08.001
41. Lim HB, Kim YW, Kim JM et al (2018) the importance of signal strength in quantitative assessment of retinal vessel density using optical coherence tomography angiography. Sci Rep 8(1):12897. https://doi.org/10.1038/s41598-018-31321-9
42. Czakó C, István L, Benyó F, Ál É et al (2020) The impact of deterministic signal loss on OCT angiography measurements. Transl Vis Sci Technol 9(5):10. https://doi.org/10.1167/tvst.9.5.10